

Multipole Susceptibility of Multiorbital Anderson Model Coupled with Jahn-Teller Phonons

Takashi HOTTA

Advanced Science Research Center, Japan Atomic Energy Agency, Tokai, Ibaraki 319-1195

(Received April 14, 2018)

In order to clarify possible multipole states of Sm-based filled skutterudite compounds, we investigate multipole susceptibility of a multiorbital Anderson model dynamically coupled with Jahn-Teller phonons by using a numerical renormalization group method. Here we take a procedure to maximize the multipole susceptibility matrix to determine the multipole state. When the electron-phonon coupling term is simply ignored, it is found that the dominant multipole state is characterized by $2u$ octupole for the Γ_{67}^- quartet ground state, while the low-temperature phase is governed by magnetic fluctuations for the Γ_5^- doublet ground state. When we include the coupling between f electrons in degenerate $\Gamma_{67}^- (e_u)$ orbitals and Jahn-Teller phonons with E_g symmetry, the mixed multipole state with $4u$ magnetic and $5u$ octupole moments is found to be dominant with significant $3g$ quadrupole fluctuations at low temperatures.

KEYWORDS: Multipole, Dynamical Jahn-Teller phonons, Sm-based filled skutterudites

1. Introduction

Recently, f -electron compounds including plural number of f electrons per ion have attracted renewed attention due to emergence of exotic magnetism and unconventional superconductivity in the research field of condensed matter physics.¹ In particular, filled skutterudite compounds, expressed as RT_4X_{12} with rare-earth atom R, transition metal atom T, and pnictogen X, have been focused, since this material group provides us a platform for systematic research of magnetism and superconductivity of f^n -electron systems with $n \geq 2$,^{2,3} where n denotes the number of f electrons.

Among various kinds of RT_4X_{12} , interesting results have been reported for Sm-based filled skutterudites. $SmRu_4P_{12}$ is known to exhibit a metal-insulator (MI) transition at $T_{MI}=16.5$ K,⁴ which is confirmed to be second order from the specific heat measurement.⁵ Further works have revealed that the MI transition occurs in two steps.⁵⁻⁷ Namely, we find three states in the phase diagram for $SmRu_4P_{12}$ in the plane of temperature and magnetic field.⁵ The phase I ($T > T_{MI}$) is paramagnetic, while the phase III is considered to be antiferromagnetic ordered state from NMR measurements.^{8,9}

Concerning the phase II between the phases I and III, an intriguing possibility of octupole ordering has been proposed by Yoshizawa *et al.* from the elastic constant measurement, showing the breaking of time reversal symmetry in the phase II.¹⁰ Recent muon spin relaxation measurement is consistent with this octupole scenario, since the static internal field has been found to grow at T_{MI} .¹¹ NMR measurement of ^{31}P has also suggested that the static internal field occurs below T_{MI} and the anomalous variation of the internal field is considered to be the evidence of the ordering of octupole.^{9,12}

In order to understand why such exotic octupole ordering appears, it is important to clarify the CEF ground state. From the specific heat measurement, for $SmRu_4P_{12}$ and $SmOs_4P_{12}$, the CEF ground state is Γ_{67}^- quartet,¹³ consistent with theoretical calculation of the CEF energy level of T_h group.¹⁴ Note that Γ_{67}^- in T_h group is equal to Γ_8^- in O_h .¹⁵ However, the CEF energy scheme seems to be changed even among the same Sm-based filled skutterudites. In fact, for $SmFe_4P_{12}$, Γ_5^- doublet ground state has been suggested.^{13,16} For $SmOs_4Sb_{12}$, it has been found to be Γ_{67}^- quartet in Ref. 17, while the CEF

ground state was considered to be Γ_5^- doublet in Ref. 18. Quite recently, magnetization measurement has been performed and the observed anisotropy seems to confirm the Γ_{67}^- quartet ground state in $SmOs_4Sb_{12}$.¹⁹

Another interesting topic on Sm-based filled skutterudites is magnetically robust heavy-fermion behavior in $SmOs_4Sb_{12}$.¹⁷ It has been suggested that this peculiar phenomenon is due to the non-magnetic Kondo effect originating from phononic degrees of freedom.²⁰ Since rare-earth ion is surrounded by the cage composed of twelve pnictogens in filled skutterudites, there is a possibility that rare-earth ion moves around potential minima in off-center positions inside the pnictogen cage. This is called the rattling, which is considered to be one of important ingredients with significant influence on electronic properties of filled skutterudites. As a natural extension of two-level Kondo problem,^{21,22} Hattori *et al.* have analyzed four- and six-level Kondo models.^{23,24} Their results seem to explain the magnetically robust heavy-fermion behavior in $SmOs_4Sb_{12}$. Concerning the positions of potential minima, neutron scattering experiment for $PrOs_4Sb_{12}$ has indicated that the charge distribution of Pr ion extends in the [1,1,1] direction at high temperatures,²⁵ suggesting that the eight-level Kondo model should be discussed.

Regarding the problem of rattling, there is another important aspect of geometrical degree of freedom. From the measurement of elastic constant, it has been suggested that the off-center motion has degenerate E_g symmetry.²⁶ Inspired by this suggestion, the present author has considered a multiorbital Anderson model with a linear coupling between degenerate f -electron orbitals with e_u symmetry and dynamical Jahn-Teller phonons with E_g symmetry.²⁷ Numerical analysis of this model for $n=2$ has revealed that quasi-Kondo behavior occurs due to the release of an entropy $\log 2$ of the vibronic ground state, originating from the clockwise and anti-clockwise rotational modes of dynamical Jahn-Teller phonons.²⁸ Such geometrical degree of freedom does not depend on the detail of potential minima, since only the rotational direction becomes important. It is interesting to pursue a possibility of Kondo-like behavior due to the dynamical Jahn-Teller effect in filled skutterudites.

In this paper, we discuss multipole properties of Sm-based

filled skutterudites on the basis of the multiorbital Anderson model. First we introduce the effective local f -electron model obtained by the expansion in terms of $1/\lambda$ based on a j - j coupling scheme,²⁹ where λ is the spin-orbit coupling. It is found that the ground state is changed between Γ_5^- doublet and Γ_{67}^- quartet, depending on Coulomb interaction and/or spin-orbit coupling. This fact is consistent with a possible change of the CEF ground state in $\text{SmT}_4\text{X}_{12}$. Then, we numerically analyze the multiorbital Anderson model. When the ground state is Γ_{67}^- quartet, the dominant multipole state is characterized by $2u$ octupole. For the Γ_5^- doublet ground state, the low-temperature phase is governed by magnetic fluctuations. When we consider the coupling with Jahn-Teller phonons, the mixed multipole state with $4u$ magnetic and $5u$ octupole moments becomes dominant at low temperatures and quadrupole fluctuations are also significant.

The organization of this paper is as follows. In §2, we introduce the effective model which describes well the low-energy local f -electron states. On the basis of the model, we discuss the CEF energy levels of Sm^{3+} from the viewpoint of the competition between Coulomb interaction and spin-orbit coupling. In §3, the multiorbital Anderson model is defined and we explain the quantities to be measured and the method of calculation. In §4, we show numerical results for the cases without and with Jahn-Teller phonons. In particular, the dominant multipole states are explained in detail. Finally, in §5, we discuss relevance of the present results to actual Sm-based filled skutterudites. Throughout this paper, we use such units as $\hbar=k_B=1$ and the energy unit is set as eV.

2. Local f -electron State

2.1 Local effective model

The local f -electron Hamiltonian is given by¹⁴

$$H_{\text{loc}} = H_{\text{so}} + H_{\text{int}} + H_{\text{CEF}}, \quad (1)$$

where H_{so} is the spin-orbit coupling term, given by

$$H_{\text{so}} = \lambda \sum_{m,\sigma,m',\sigma'} \zeta_{m,\sigma,m',\sigma'} f_{m\sigma}^\dagger f_{m'\sigma'}. \quad (2)$$

Here λ is the spin-orbit coupling and $f_{m\sigma}$ denotes the annihilation operator for f electron with spin σ and angular momentum $m(=-3, \dots, 3)$ and $\sigma=+1$ (-1) for up (down) spin. The matrix elements are expressed by

$$\begin{aligned} \zeta_{m,\sigma,m,\sigma} &= m\sigma/2, \\ \zeta_{m+\sigma,-\sigma,m,\sigma} &= \sqrt{12 - m(m+\sigma)}/2, \end{aligned} \quad (3)$$

and zero for other cases.

The second term H_{int} indicates the Coulomb interactions among f electrons, expressed by

$$H_{\text{int}} = \sum_{\substack{m_1 \sim m_4 \\ \sigma_1, \sigma_2}} I_{m_1, m_2, m_3, m_4} f_{m_1 \sigma_1}^\dagger f_{m_2 \sigma_2}^\dagger f_{m_3 \sigma_2} f_{m_4 \sigma_1}, \quad (4)$$

where the Coulomb integral I_{m_1, m_2, m_3, m_4} is given by

$$I_{m_1, m_2, m_3, m_4} = \sum_{k=0}^6 F^k c_k(m_1, m_4) c_k(m_2, m_3). \quad (5)$$

Note that the sum is limited by the Wigner-Eckart theorem to even values ($k=0, 2, 4,$ and 6). Here F^k is the radial integral for the k -th partial wave, called Slater integral or Slater-Condon parameter^{30,31} and c_k is the Gaunt coefficient.^{32,33}

The Slater-Condon parameters and the spin-orbit interaction are determined so as to reproduce the spectra of rare-earth and actinide ions for each value of n , but the Slater-Condon parameters are considered to be distributed among 1 eV and 10 eV, while λ is in the order of 0.1 eV. In this paper, for convenience, we parameterize F^k as

$$F^0 = 10U, \quad F^2 = 5U, \quad F^4 = 3U, \quad F^6 = U, \quad (6)$$

where U denotes the order of the Hund's rule interaction among f orbitals, which is in the order of a few eV.

The CEF term H_{CEF} is given by

$$H_{\text{CEF}} = \sum_{m,m',\sigma} B_{m,m'} f_{m\sigma}^\dagger f_{m'\sigma}, \quad (7)$$

where $B_{m,m'}$ is determined from the table of Hutchings for angular momentum $J=\ell=3$,³⁴ since we are now considering the potential for f electron. For filled skutterudites with T_h symmetry,¹⁵ $B_{m,m'}$ is expressed by using three CEF parameters B_4^0 , B_6^0 , and B_6^2 as

$$\begin{aligned} B_{3,3} &= B_{-3,-3} = 180B_4^0 + 180B_6^0, \\ B_{2,2} &= B_{-2,-2} = -420B_4^0 - 1080B_6^0, \\ B_{1,1} &= B_{-1,-1} = 60B_4^0 + 2700B_6^0, \\ B_{0,0} &= 360B_4^0 - 3600B_6^0, \\ B_{3,-1} &= B_{-3,1} = 60\sqrt{15}(B_4^0 - 21B_6^0), \\ B_{2,-2} &= 300B_4^0 + 7560B_6^0, \\ B_{3,1} &= B_{-3,-1} = 24\sqrt{15}B_6^2, \\ B_{2,0} &= B_{-2,0} = -48\sqrt{15}B_6^2, \\ B_{1,-1} &= -B_{3,-3} = 360B_6^2. \end{aligned} \quad (8)$$

Note the relation of $B_{m,m'}=B_{m',m}$. Following the traditional notation, we define

$$\begin{aligned} B_4^0 &= Wx/F(4), \\ B_6^0 &= W(1 - |x|)/F(6), \\ B_6^2 &= Wy/F^t(6), \end{aligned} \quad (9)$$

where x and y specify the CEF scheme for T_h point group, while W determines an energy scale for the CEF potential. Concerning $F(4)$, $F(6)$, and $F^t(6)$, we choose $F(4)=15$, $F(6)=180$, and $F^t(6)=24$ for $\ell=3$.^{34,35} In actual f -electron materials, the magnitude of the CEF potential is considered to be $10^{-4} \sim 10^{-3}$ eV. For the calculation of the CEF energy level in this paper, we set $W = -6 \times 10^{-4}$ eV.

Although H_{loc} provides us correct CEF ground states irrespective of the number of f electrons and other parameters, it is difficult to consider multipole properties and the effect of Jahn-Teller phonons. In order to make further steps, it is convenient to employ the j - j coupling scheme.³⁶ Namely, we accommodate f electrons in the $j=5/2$ sextet by considering the CEF potential and Coulomb interactions. An advantage of the j - j coupling scheme is that we can take into account many-body effects using standard quantum-field theoretical techniques, since individual f -electron states are clearly defined. Then, we have developed microscopic theories for magnetism and superconductivity on the basis of the j - j coupling scheme by focusing on the potential roles of f -electron orbitals.³⁷⁻⁴⁵ In particular, it is also possible to develop microscopic theory for multipole ordering and fluctuations.⁴⁶⁻⁵¹

However, since the sixth order CEF terms cannot be included in the $j=5/2$ sextet due to the symmetry reason, contributions of B_6^0 and B_6^2 are dropped in the simple j - j coupling scheme. It has been a disadvantage of the j - j coupling

scheme that the effect of B_6^2 , which is characteristic of T_h symmetry, cannot be included. In order to improve the situation, recently, the modified j - j coupling has been developed so as to include the effect of B_6^0 and B_6^2 terms in the order of $1/\lambda$ due to the degenerate perturbation theory.²⁹ The modified j - j coupling scheme can correctly reproduce the CEF energy levels for $n \geq 2$ in the realistic intermediate coupling region with λ/U in the order of 0.1.

In order to obtain the effective model H_{eff} , we treat $H_{\text{CEF}} + H_{\text{int}}$ as a perturbation to H_{SO} . The details are explained in Ref. 29. Here we show H_{eff} as

$$H_{\text{eff}} = \sum_{\mu, \nu} \tilde{B}_{\mu, \nu} f_{\mu}^{\dagger} f_{\nu} + \sum_{\mu_1 \sim \mu_4} \tilde{I}_{\mu_1 \mu_2, \mu_3 \mu_4} f_{\mu_1}^{\dagger} f_{\mu_2}^{\dagger} f_{\mu_3} f_{\mu_4}, \quad (10)$$

where f_{μ} is the annihilation operator for f electron with angular momentum $\mu (= -5/2, \dots, 5/2)$ in the $j=5/2$ sextet. The modified CEF potential is expressed as

$$\tilde{B}_{\mu, \nu} = \tilde{B}_{\mu, \nu}^{(0)} + \tilde{B}_{\mu, \nu}^{(1)}, \quad (11)$$

where $\tilde{B}_{\mu, \nu}^{(0)}$ denotes the CEF potential for $J=5/2$ and $\tilde{B}_{\mu, \nu}^{(1)}$ is the correction in the order of W^2/λ . The effective interaction in eq. (10) is given by

$$\tilde{I}_{\mu_1, \mu_2, \mu_3, \mu_4} = \tilde{I}_{\mu_1, \mu_2, \mu_3, \mu_4}^{(0)} + \tilde{I}_{\mu_1, \mu_2, \mu_3, \mu_4}^{(1)}, \quad (12)$$

where $\tilde{I}_{\mu_1, \mu_2, \mu_3, \mu_4}^{(0)}$ is expressed by three Racah parameters, E_0 , E_1 , and E_2 , which are related to the Slater-Condon parameters as

$$\begin{aligned} E_0 &= F^0 - (80/1225)F^2 - (12/441)F^4, \\ E_1 &= (120/1225)F^2 + (18/441)F^4, \\ E_2 &= (12/1225)F^2 - (1/441)F^4. \end{aligned} \quad (13)$$

Explicit expressions of $\tilde{I}^{(0)}$ are shown in Ref. 36. On the other hand, $\tilde{I}_{\mu_1, \mu_2, \mu_3, \mu_4}^{(1)}$ is the correction term in the order of $1/\lambda$.

Here, four comments are in order. (i) Effects of B_6^0 and B_6^2 are included as two-body potentials in $\tilde{I}^{(1)}$. (ii) The lowest-order energy of $\tilde{I}^{(1)}$ is $|W|U/\lambda$. (iii) The effective model is valid for f -electron compounds with the hybridization V smaller than λ . (iv) The parameter space in which H_{eff} works is determined by the conditions for the weak CEF, i.e., $|W|/U \ll 1$ and $|W|U/\lambda \ll E_2$. Concerning the value of λ , we obtain $|W|/\lambda \ll 0.02$ from eqs. (6) and (13). Note that E_2 plays a role of the effective Hund's rule interaction in the j - j coupling scheme, estimated as $E_2 \sim J_{\text{H}}/49$.²⁹ Thus, it is allowed to use H_{eff} even for λ in the order of 0.1 eV, when $|W|$ is set as a realistic value in the order of 10^{-4} eV for actual f -electron materials.

2.2 CEF energy schemes

In order to determine the CEF parameters of filled skutterudite compounds, first let us consider the CEF energy level for the case of $n=2$. A typical material is $\text{PrOs}_4\text{Sb}_{12}$. From experimental results on specific heat,⁵² magnetization,⁵³ and neutron scattering,⁵⁴⁻⁵⁶ it has been confirmed that the ground state of $\text{PrOs}_4\text{Sb}_{12}$ is Γ_1^+ singlet, while the first excited state is $\Gamma_4^{+(2)}$ triplet with very small excitation energy ($\sim 10\text{K}$).

In Fig. 1(a), we show the CEF energy levels of H_{eff} for the case of $n=2$. Here we set $\lambda=0.1$, $U=1$, $W=-6 \times 10^{-4}$, and $y=0.3$, which are considered to be realistic values for Pr-based filled skutterudites. Here the minus sign is added in W so as to be consistent with the appearance of Γ_1^+ singlet ground

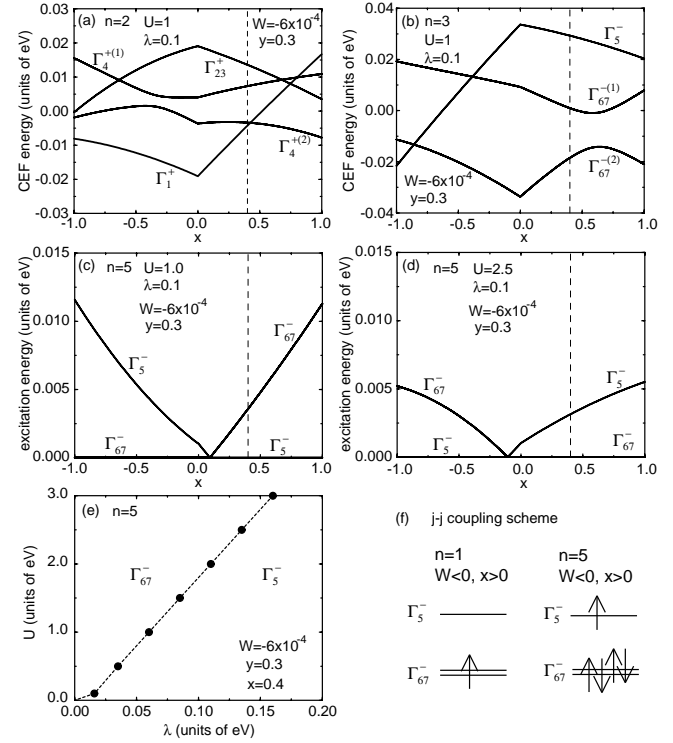


Fig. 1. CEF energy levels of H_{eff} for (a) $n=2$ and $U=1$, (b) $n=3$ and $U=1$, (c) $n=5$ and $U=1$, and (d) $n=5$ and $U=2.5$. We set $\lambda=0.1$, $W=-6 \times 10^{-4}$, and $y=0.3$ for (a)-(d). (e) Phase diagram of the CEF ground state of H_{eff} for $n=5$, $W=-6 \times 10^{-4}$, $x=0.4$, and $y=0.3$. (f) Electron configurations for $n=1$ and 5 in the j - j coupling scheme for $B_4^0 < 0$.

state. It should be noted that two triplet states in O_h , Γ_4^+ and Γ_5^+ , are mixed as $\Gamma_4^{+(1)}$ and $\Gamma_4^{+(2)}$ in T_h . As understood from Fig. 1(a), $x=0.4$ seems to correspond to the actual situation of $\text{PrOs}_4\text{Sb}_{12}$, since the CEF excitation energy is 1 meV, which is consistent with experimental results.

Now we substitute the rare-earth ion from Pr^{3+} ($n=2$) to Nd^{3+} ($n=3$) and Sm^{3+} ($n=5$). Here we note that in principle, it is not necessary to change the CEF parameters even when rare-earth ion is substituted, since the CEF potential is given by the sum of electrostatic potentials from ligand ions. Then, it is reasonable to use the same CEF parameters also for $\text{NdOs}_4\text{Sb}_{12}$ and $\text{SmOs}_4\text{Sb}_{12}$. In actuality, the electrostatic potential may be changed depending on the ion radius of R and/or the kinds of T and X. In this sense, x , y , and the absolute value of $|W|$ may be changed among filled skutterudite compounds, but there is no reason to change the sign of W . Throughout this paper, we keep W as negative.

Let us discuss the CEF states for $n=3$.⁵⁷ In Fig. 1(b), we show the CEF energy levels of H_{loc} for $n=3$ by using the same parameters as in Fig. 1(a). At $x=0.4$, the ground state is Γ_{67}^- quartet and the excited state is another Γ_{67}^- quartet, consistent with the experimental result for $\text{NdOs}_4\text{Sb}_{12}$.⁵⁸ As for the CEF excitation energy, it is 0.02eV in the present calculation, while it has been experimentally estimated as 220K.⁵⁸ We can obtain the CEF energy for $\text{NdOs}_4\text{Sb}_{12}$ consistent with the experimental result by using the CEF parameters of $\text{PrOs}_4\text{Sb}_{12}$.

In Fig. 1(c), we show the CEF states for $n=5$ by using the same parameters as in Fig. 1(a). Since we obtain two multiplets, Γ_5^- and Γ_{67}^- , for $n=5$, it is convenient to draw the excitation energy. At $x=0.4$, the ground state is Γ_5^- doublet,

while the experimental result for $\text{SmOs}_4\text{Sb}_{12}$ has suggested Γ_{67}^- quartet ground state.¹⁷ Here we note that the values of U and λ can be different for different rare-earth ions. In the cases of $n=2$ and $n=3$, even if U and λ are changed within the realistic range, the CEF energy scheme does not change qualitatively. However, this is not the case for $n=5$.

In Fig. 1(d), we show the results of the CEF energy levels for $U=2.5$ and $\lambda=0.1$ by using the same CEF parameters as in Fig. 1(c). It is observed that the x dependence is reversed from that in Fig. 1(c), suggesting that the CEF ground state is changed, even though we do not change the CEF parameters. At $x=0.4$, the ground state is Γ_{67}^- quartet and the excitation energy is about 3 meV in the present calculation, which is comparable with the experimental value of 19K.¹⁷

We note that the conversion of the ground state by the change of U (or λ) is *not* due to the approximation of H_{eff} , but an intrinsic feature of f electrons, since we could find the same results when we diagonalize simultaneously CEF potential, Coulomb interaction, and spin-orbit coupling.²⁹ By changing U and λ , we depict the phase diagram for the CEF ground state for the case of $n=5$ and $x=0.4$, as shown in Fig. 1(e). Note that in the region of very small λ , H_{eff} does not work, but it is still available for $\lambda \gg 0.015$ for the present parameter choice. Roughly speaking, for large λ and small U , the ground state is Γ_{67}^- quartet, while for small λ and large U , Γ_5^- doublet is the ground state.

In order to understand the change of the CEF ground state, it is useful to consider the two limiting situations, $\lambda \ll U$ and $\lambda \gg U$, corresponding to the LS and $j-j$ coupling schemes, respectively. First we consider the case of the LS coupling scheme. The relevant CEF parameter is B_4^0 , which is expressed as $B_4^0 = A_4 \beta_J(n) \langle r^4 \rangle$, where A_4 is a parameter depending on materials, $\beta_J(n)$ is the so-called Stevens factor, appearing in the method of operator equivalent,⁵⁹ and $\langle r^4 \rangle$ indicates the radial average concerning the local f -electron wavefunction. When we assume that A_4 is invariant in the same material group and $\langle r^4 \rangle$ does not depend on the f -electron number, the CEF parameter is basically determined by $\beta_J(n)$, which depend on n , U , and λ .²⁹

In the LS coupling scheme, $\beta_{5/2}(1) = (11/7)\beta_\ell$ and $\beta_{5/2}(5) = (13/21)\beta_\ell$, where $\beta_\ell = \beta_3(1) = 2/495$ for $\ell=3$. Note that $\beta_{5/2}(n)$ is different between the cases of $n=1$ and 5 even for the same $J=5/2$, since $L=3$ and $S=1/2$ for $n=1$, while $L=5$ and $S=5/2$ for $n=5$, where L and S are total angular momentum and spin momentum, respectively. Namely, in the LS coupling scheme, B_4^0 should have the same sign for $n=1$ and 5. The CEF ground state for $n=1$ is Γ_5^- doublet for $B_4^0 > 0$, while it is Γ_{67}^- quartet for $B_4^0 < 0$. Thus, in the LS coupling scheme, it is easy to understand that the ground state for $n=5$ is the Γ_{67}^- quartet in the region of $x > 0$ for the present parameterization of $B_4^0 = Wx/15$ with negative W .

Next let us consider another limiting case corresponding to the $j-j$ coupling scheme, in which we simply accommodate electrons in the one-electron potentials,³⁶ as shown in Fig. 1(f). For $x > 0$ with $W < 0$, i.e., negative B_4^0 , we put five electrons in the level scheme of lower Γ_{67}^- and higher Γ_5^- . Thus, we immediately understand that the ground state becomes Γ_5^- doublet for $n=5$ in the $j-j$ coupling scheme, when Γ_{67}^- quartet is the ground state for $n=1$. In fact, in the $j-j$ coupling scheme, we obtain $\beta_{5/2}(1) = (11/7)\beta_\ell$ and $\beta_{5/2}(5) = (-11/7)\beta_\ell$. The sign of B_4^0 is different between the

cases of $n=1$ and 5 in the $j-j$ coupling scheme. When we change the values of U and/or λ from the LS to $j-j$ coupling regions, we can find the smooth change of $\beta_{5/2}(5)$ from $(13/21)\beta_\ell$ to $(-11/7)\beta_\ell$, as found in Ref. 29

The present result suggests a “non-CEF” scenario to understand the change of the CEF ground state in Sm-based filled skutterudites. As mentioned in the introduction, for $\text{SmRu}_4\text{P}_{12}$ and $\text{SmOs}_4\text{P}_{12}$, the CEF ground state is Γ_{67}^- quartet, while the ground state of $\text{SmFe}_4\text{P}_{12}$ is Γ_5^- doublet. In order to explain the change of the ground state within the LS coupling scheme, it is necessary to change the sign of B_4^0 . The magnitude of the CEF potential may be changed due to the difference in the ion radius of R and the substitution of T and/or X in RT_4X_{12} , but it seems difficult to imagine that the sign of the CEF potential is changed among $\text{SmT}_4\text{X}_{12}$. As understood from Fig. 1(e), it is observed that the ground state conversion occurs around the region for realistic values of λ and U . Namely, due to the change in U and/or λ , the ground state is easily interchanged for actual Sm materials.

3. Model and Method

3.1 Multiorbital Anderson Hamiltonian

From the band-structure calculations, it has been revealed that the main conduction band of filled skutterudites is a_u with xyz symmetry,⁶⁰ which is hybridized with f electrons in the Γ_5^- state with a_u symmetry. In order to specify the f -electron state, we introduce “orbital” index which distinguishes three kinds of the Kramers doublets, two Γ_{67}^- and one Γ_5^- . Here “a” and “b” denote the two Γ_{67}^- 's and “c” indicates the Γ_5^- .

Then, the multiorbital Anderson model is given by

$$H = \sum_{\mathbf{k}\sigma} \varepsilon_{\mathbf{k}} c_{\mathbf{k}\sigma}^\dagger c_{\mathbf{k}\sigma} + \sum_{\mathbf{k}\sigma} (V c_{\mathbf{k}\sigma}^\dagger f_{c\sigma} + \text{h.c.}) + H_{\text{eff}} + H_{\text{eph}}, \quad (14)$$

where $\varepsilon_{\mathbf{k}}$ is the dispersion of a_u conduction electrons with Γ_5^- symmetry, $f_{\gamma\sigma}$ is the annihilation operator of f electrons on the impurity site with pseudospin and orbital γ , $c_{\mathbf{k}\sigma}$ is the annihilation operator for conduction electrons with momentum \mathbf{k} and pseudo-spin σ , and V is the hybridization between conduction and f electrons with a_u symmetry. Throughout this paper, we set $V=0.05$ eV. Note that the energy unit of H is half of the bandwidth of the conduction band, which is considered to be in the order of 1 eV, since the bandwidth has been typically estimated as 2.7 eV for $\text{PrRu}_4\text{P}_{12}$.⁶¹ Thus, the energy unit of H is taken as eV. To set the local f -electron number as $n=5$, we adjust the f -electron chemical potential.

The last term in eq. (14) denotes the electron-phonon coupling. Here, the effect of E_g rattling is included as relative vibration of surrounding atoms. We remark that localized Γ_{67}^- orbitals with e_u symmetry have linear coupling with JT phonons with E_g symmetry, since the symmetric representation of $e_u \times e_u$ includes E_g . Then, H_{eph} is given by

$$H_{\text{eph}} = g(Q_2\tau_x + Q_3\tau_z) + (P_2^2 + P_3^2)/2 + (\omega^2/2)(Q_2^2 + Q_3^2) + b(Q_3^3 - 2Q_2^2Q_3), \quad (15)$$

where g is the electron-phonon coupling constant, Q_2 and Q_3 are normal coordinates for $(x^2 - y^2)$ - and $(3z^2 - r^2)$ -type JT phonons, respectively, P_2 and P_3 are corresponding canonical momenta, $\tau_x = \sum_{\sigma} (f_{a\sigma}^\dagger f_{b\sigma} + f_{b\sigma}^\dagger f_{a\sigma})$, $\tau_z = \sum_{\sigma} (f_{a\sigma}^\dagger f_{a\sigma} -$

$f_{b\sigma}^\dagger f_{b\sigma}$), ω is the frequency of local JT phonons, and b indicates the cubic anharmonicity. Note that the reduced mass for JT modes is set as unity. Here we introduce non-dimensional electron-phonon coupling constant α and the anharmonic energy β as $\alpha=g^2/(2\omega^3)$ and $\beta=b/(2\omega)^{3/2}$, respectively.

3.2 Multipole Susceptibility

In order to clarify the magnetic properties at low temperatures, we usually discuss the magnetic susceptibility, but in more general, it is necessary to consider the susceptibility of multipole moments such as dipole, quadrupole, and octupole.⁶² The multipole operator is given in the second-quantized form as

$$X_\gamma = \sum_{\mu,\nu} (X_\gamma)_{\mu\nu} f_\mu^\dagger f_\nu, \quad (16)$$

where X denotes the symbol of multipole with the symmetry of Γ_γ and γ indicates a set of indices for the irreducible representation. For $j=5/2$, we can define multipole operators up to rank 5 in general, but we are interested in multipole properties from the Γ_8 quartet. Thus, we concentrate on multipole moments up to rank 3.

Now let us show explicit forms for multipole operators following Ref. 63. See also Ref. 62. As for dipole moments with Γ_{4u} symmetry, we express the operators as

$$J_{4ux} = J_x, \quad J_{4uy} = J_y, \quad J_{4uz} = J_z, \quad (17)$$

where J_x , J_y , and J_z are three angular momentum operators for $j=5/2$, respectively. Concerning quadrupole moments, they are classified into Γ_{3g} and Γ_{5g} . We express Γ_{3g} quadrupole operators as

$$\begin{aligned} O_{3gu} &= (2J_z^2 - J_x^2 - J_y^2)/2, \\ O_{3gv} &= \sqrt{3}(J_x^2 - J_y^2)/2. \end{aligned} \quad (18)$$

For the Γ_{5g} quadrupole, we have the three operators

$$\begin{aligned} O_{5g\xi} &= \sqrt{3} J_y J_z / 2, \\ O_{5g\eta} &= \sqrt{3} J_z J_x / 2, \\ O_{5g\zeta} &= \sqrt{3} J_x J_y / 2, \end{aligned} \quad (19)$$

where the bar denotes the operation of taking all possible permutations in terms of cartesian components.

Regarding octupole moments, there are three types as Γ_{2u} , Γ_{4u} , and Γ_{5u} . We express the Γ_{2u} octupole as

$$T_{2u} = \sqrt{15} J_x J_y J_z / 6. \quad (20)$$

For the Γ_{4u} octupole, we express the operators as

$$\begin{aligned} T_{4ux} &= (2J_x^3 - \overline{J_x J_y^2} - \overline{J_x J_z^2})/2, \\ T_{4uy} &= (2J_y^3 - \overline{J_y J_z^2} - \overline{J_y J_x^2})/2, \\ T_{4uz} &= (2J_z^3 - \overline{J_z J_x^2} - \overline{J_z J_y^2})/2, \end{aligned} \quad (21)$$

while the Γ_{5u} octupole operators are given by

$$\begin{aligned} T_{5ux} &= \sqrt{15} (\overline{J_x J_y^2} - \overline{J_x J_z^2})/6, \\ T_{5uy} &= \sqrt{15} (\overline{J_y J_z^2} - \overline{J_y J_x^2})/6, \\ T_{5uz} &= \sqrt{15} (\overline{J_z J_x^2} - \overline{J_z J_y^2})/6. \end{aligned} \quad (22)$$

We redefine the multipole moments so as to satisfy the orthonormal condition $\text{Tr}(X_\gamma X_{\gamma'}) = \delta_{\gamma\gamma'}$,⁶⁴ where $\delta_{\gamma\gamma'}$ is the Kronecker's delta.

In principle, the multipole susceptibility can be evaluated in the linear response theory,⁶² but we should note that the

multipole moments belonging to the same symmetry can be mixed in general. In order to determine the coefficient of such mixed multipole moment, it is necessary to find the optimized multipole state which maximizes the susceptibility. Namely, we define the multipole operator as

$$M = \sum_{\gamma} p_{\gamma} X_{\gamma}, \quad (23)$$

where p_{γ} is determined by the eigenstate with the maximum eigenvalue of the susceptibility matrix, given by

$$\chi_{\gamma\gamma'} = \frac{1}{Z} \sum_{n,m} \frac{e^{-E_n/T} - e^{-E_m/T}}{E_m - E_n} \langle n | X_{\gamma} | m \rangle \langle m | X_{\gamma'} | n \rangle, \quad (24)$$

where E_n is the eigenenergy for the n -th eigenstate $|n\rangle$ and Z is the partition function given by $Z = \sum_n e^{-E_n/T}$.

3.3 Method

In order to evaluate multipole susceptibilities, here we employ a numerical renormalization group (NRG) method,^{65,66} in which momentum space is logarithmically discretized to include efficiently the conduction electrons near the Fermi energy and the conduction electron states are characterized by ‘‘shell’’ labeled by N . The shell of $N=0$ denotes an impurity site described by the local Hamiltonian. The Hamiltonian is transformed into the recursion form as

$$H_{N+1} = \sqrt{\Lambda} H_N + t_N \sum_{\sigma} (c_{N\sigma}^\dagger c_{N+1\sigma} + c_{N+1\sigma}^\dagger c_{N\sigma}), \quad (25)$$

where Λ is a parameter for logarithmic discretization, $c_{N\sigma}$ denotes the annihilation operator of conduction electron in the N -shell, and t_N indicates ‘‘hopping’’ of electron between N - and $(N+1)$ -shells, expressed by

$$t_N = \frac{(1 + \Lambda^{-1})(1 - \Lambda^{-N-1})}{2\sqrt{(1 - \Lambda^{-2N-1})(1 - \Lambda^{-2N-3})}}. \quad (26)$$

The initial term H_0 is given by

$$H_0 = \Lambda^{-1/2} [H_{\text{eff}} + H_{\text{eph}} + \sum_{\sigma} V (c_{0\sigma}^\dagger f_{c\sigma} + f_{c\sigma}^\dagger c_{0\sigma})]. \quad (27)$$

The component of multipole susceptibility eq. (24) is evaluated by using the renormalized state. The free energy F for f electron is evaluated by

$$F = -T \lim_{N \rightarrow \infty} \left[\ln \text{Tr} e^{-H_N/T} - \ln \text{Tr} e^{-H_N^0/T} \right]. \quad (28)$$

Note that the temperature T is defined as $T = \Lambda^{-(N-1)/2}$ in the NRG calculation. The entropy S_{imp} is obtained by $S_{\text{imp}} = -\partial F / \partial T$ and the specific heat C_{imp} is evaluated by $C_{\text{imp}} = -T \partial^2 F / \partial T^2$. In this paper, Λ is set as 5 and we keep 3000 low-energy states for each renormalization step. The phonon basis for each JT mode is truncated at a finite number N_{ph} , which is set as $N_{\text{ph}}=20$.

4. Results

4.1 Without Jahn-Teller phonons

First let us consider the case without H_{eph} . In Fig. 2(a), we show the multipole susceptibility χ for $U=1$ and $\lambda=0.1$ with the Γ_5^- ground state. At low temperatures, we find the 4u magnetic state and other multipoles are suppressed. Note that the 4u magnetic moment is expressed as

$$M_{4ua} = p_a J_{4ua} + q_a T_{4ua}, \quad (29)$$

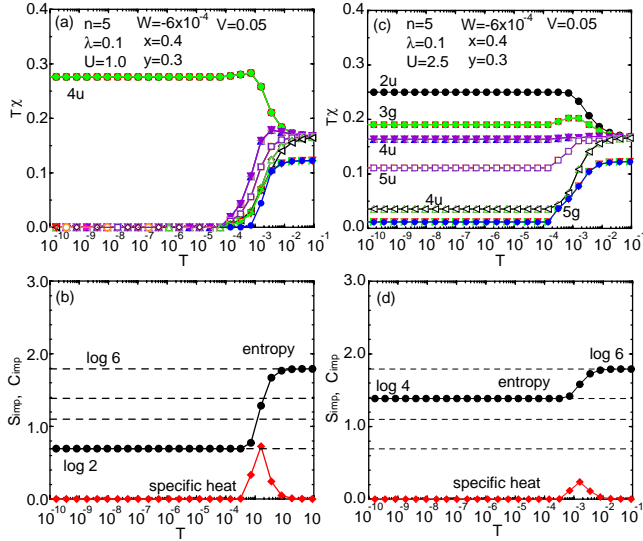


Fig. 2. (a) $T\chi$ and (b) S_{imp} and C_{imp} vs. temperature for $\lambda=0.1$ and $U=1.0$. (c) $T\chi$ and (d) S_{imp} and C_{imp} vs. temperature for $\lambda=0.1$ and $U=2.5$.

for $a=x, y$, and z , since the moments belonging in the same symmetry are mixed in general.⁶⁴ For the present parameters, we find $p_a=0.326$ and $q_a=-0.946$. As shown in Fig. 2(b), we find a residual entropy $\log 2$ of Γ_5^- doublet, but it is not the true ground state. For instance, when we increase the hybridization V , the $4u$ magnetic moment is screened even in the present temperature range. In any case, for the case of Γ_5^- ground state, there are no significant higher-order multipoles. We find the standard Kondo physics, when the extra coupling to JT phonons is not considered.

On the other hand, the low-temperature state is drastically changed, when the ground state is Γ_{67}^- quartet, as shown in Fig. 2(c). After the diagonalization of the susceptibility matrix, we obtain that the dominant multipole is purely given by $2u$ octupole. The second and third multipole states have $3g$ quadrupole and $4u$ magnetic moments, respectively. The $4u$ moment is expressed by eq. (29) with $p_a=0.560$ and $q_a=0.828$. The fourth multipole state is given by $5u$ octupole, but in the case of $n=5$, $4u$ moment is not mixed with $5u$, in contrast to the case of $n=3$.⁵⁷ As explained in the previous section for the CEF states of $n=2$, $4u$ and $5u$ states in O_h symmetry are mixed in T_h . Thus, the mixture of $4u$ and $5u$ moments is one of characteristic points of filled skutterudites with T_h symmetry. However, this mixing occurs due to the CEF term of B_6^2 , which does not appear in the $J=5/2$ space for $n=1$ and 5 . Thus, in Sm-based filled skutterudites, the mixing of $4u$ and $5u$ moments does not occur within an electronic model. In Fig. 2(c), we also find another $4u$ state and $5g$ quadrupole.

In the case of the Γ_{67}^- ground state, since this quartet carries all the multipole moments up to rank 3, we find the significant values for all moments. As shown in Fig. 2(d), we find a residual entropy of $\log 4$, corresponding to the localized Γ_{67}^- quartet, since we have considered the hybridization between a_u conduction band and Γ_5^- state. In actuality, there should exist a finite hybridization between e_u conduction bands and Γ_{67}^- states, even if the value is not large compared with that between a_u conduction and Γ_5^- electrons. Thus, the entropy of $\log 4$ should be eventually released at low temperatures in

the actual situation.

4.2 With Jahn-Teller phonons

Next we include the effect of dynamical JT phonons, but before proceeding to the numerical results, let us briefly review the effect of JT phonons in the adiabatic approximation by following Ref. 28. Note that in actuality, the potential is not static, but it dynamically changes to follow the electron motion. For $\beta=0$, the potential is continuously degenerate along the circle of the bottom of the Mexican-hat potential. Thus, we obtain double degeneracy in the vibronic state concerning the rotational JT modes along clockwise and anti-clockwise directions. When a temperature becomes lower than a characteristic energy T^* , which is related to a time scale to turn the direction of rotational JT modes, the entropy $\log 2$ should be eventually released, leading to Kondo-like behavior, since the specific rotational direction disappears due to the average over the long enough time.

In Figs. 3(a) and 3(b), we show multipole susceptibilities, entropy, and specific heat for $\omega=0.3$, $\alpha=0.5$, and $\beta=0.0$. Note that here we suppress the cubic anharmonicity. We find that all the multipole moments are still active, although the dominant multipole is changed from $2u$ to $4u$. In this sense, the results do not seem to be qualitatively changed between Figs. 2(c) and 3(a), in spite of the JT active situation. We find a residual entropy of $\log 4$ in Fig. 3(b). In Fig. 3(c), we show the temperature dependence of average displacements. For the whole temperature range, we find finite values of $\sqrt{\langle Q_2^2 \rangle}$ and $\sqrt{\langle Q_3^2 \rangle}$, while $\langle Q_2 \rangle = \langle Q_3 \rangle = 0$. Namely, JT vibrations occur around the origin without displacements. As the temperature is decreased, such vibrations are expected to be suppressed, but in the temperature range, we cannot find it. Rather, due to the isotropic JT vibrations, orbital fluctuations are still active in addition to magnetic fluctuations, leading to active multipole fluctuations.

As explained in Ref. 28, when we include the effect of anharmonicity, three potential minima appear in the bottom of the JT potential in the adiabatic approximation. Since the rotational mode should be changed to the quantum tunneling among three potential minima at low temperatures, the frequency is effectively reduced in the factor of $e^{-\delta E/\omega}$, where δE is the potential barrier. Then, we expect to observe the quasi-Kondo behavior even in the present temperature range, when we include the effect of cubic anharmonicity.

In Figs. 3(d) and 3(e), we show multipole susceptibilities, entropy, and specific heat for $\omega=0.3$, $\alpha=0.5$, and $\beta=-0.006$. For $T > 10^{-5}$, multipole susceptibilities are quite similar to Fig. 3(a). However, when temperature is decreased, the mixed multipole state with $4u$ magnetic and $5u$ octupole moments becomes dominant. This mixed moment is expressed as

$$M_a = p_a J_{4ua} + q_a T_{4ua} + r_a T_{5ua}, \quad (30)$$

for $a=x$ and y . In the low-temperature region, we obtain $p_a=0.761$, $q_a=0.428$, and $r_a=-0.488$. Due to the effect of JT phonons, we find a significant contribution of $5u$ octupole. It is emphasized that the $5u$ component first appears in the present case for $n=5$. The secondary moment is given by $3gu$ quadrupole and the third state is given by

$$M_z = p_z J_{4uz} + q_z T_{4uz} + r_z T_{5uz}, \quad (31)$$

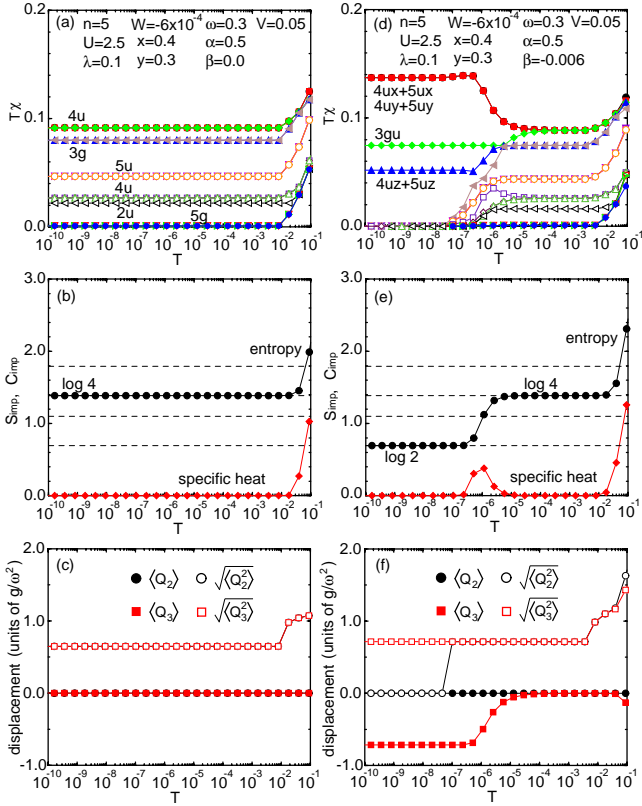


Fig. 3. (a) $T\chi$, (b) S_{imp} and C_{imp} , and (c) $\langle Q_i \rangle$ and $\sqrt{\langle Q_i^2 \rangle}$ ($i=2$ and 3) vs. temperature for $\lambda=0.1$, $U=2.5$, and $\beta=0$. (d) $T\chi$, (e) S_{imp} and C_{imp} , and (f) $\langle Q_i \rangle$ and $\sqrt{\langle Q_i^2 \rangle}$ ($i=2$ and 3) vs. temperature for $\lambda=0.2$, $U=1.0$, and $\beta=-0.006$.

where $p_z=0.67$, $q_z=-0.739$, and $r_z=0.0$. Note that r_z is found to be zero within the numerical precision, but it is difficult to conclude that it vanishes exactly.

In Fig. 3(e), around at $T=10^{-6}$, we find a peak in the specific heat, since an entropy of $\log 2$ is released. As mentioned above, this is considered to be quasi-Kondo behavior, originating from the suppression of the rotational mode of dynamical JT phonons.²⁸ In this case, an entropy of $\log 2$ concerning orbital degree of freedom coupled with JT phonons is released, while there still remains spin degree of freedom in the localized Γ_{67}^- quartet. In fact, at low temperatures, magnetic susceptibility becomes dominant.

In Fig. 3(f), we show the temperature dependence of average displacements. For $T>10^{-6}$, we find $\sqrt{\langle Q_2^2 \rangle} \neq 0$ and $\sqrt{\langle Q_3^2 \rangle} \neq 0$, suggesting that both Q_2 and Q_3 modes are active. This is consistent with the finite values of susceptibilities for O_{3gu} and O_{3gv} . Note that the displacement is not considered to occur, since $\langle Q_2 \rangle = \langle Q_3 \rangle = 0$. In the low-temperature region, after the release of an entropy $\log 2$ of the rotational degree of freedom, we find $\sqrt{\langle Q_2^2 \rangle} = \langle Q_2 \rangle = 0$, while $\sqrt{\langle Q_3^2 \rangle} = |\langle Q_3 \rangle| \neq 0$, indicating that only Q_3 -type JT vibration is active with finite displacement. This is also consistent with the result that χ_{3gu} remains at low temperatures, since the vibration mode is fixed as Q_3 -type, after the quasi-Kondo phenomenon occurs. Namely, the JT vibrations become anisotropic for $T < T^*$, while they are isotropic for $T > T^*$, as mentioned in Ref. 28.

For the case with JT phonons, we have shown only the results for the Γ_{67}^- ground state. When we evaluate the mul-

tipole susceptibility, specific heat, entropy, average displacement for the Γ_{67}^- ground state, we find the results quite similar to Figs. 3. In the present parameters, the ground state character is masked due to the effect of JT phonons. If we increase the CEF excitation energy, we could find different results from those of Fig. 3 for the Γ_{67}^- ground state, but it is not so important in the context of Sm-based filled skutterudites with the CEF excitation in the order of 10K.

5. Discussion and Summary

In this paper, we have examined the multipole state of Sm-based filled skutterudites on the basis of the multiorbital Anderson model with the use of the NRG method. As mentioned in the introduction, a possibility of octupole ordering has been discussed experimentally in $\text{SmRu}_4\text{P}_{12}$.⁹⁻¹¹ In general, there are two possibilities as 2u and 5u octupoles. The 2u octupole has been found to be dominant in the electronic model, when we do not include the coupling between f electrons and JT phonons. On the other hand, the 5u octupole becomes significant in the mixed state with 4u magnetic moment, when we consider the coupling to JT phonons.

In the experiment, Yoshizawa *et al.* have suggested the 5u octupole from the elastic constant measurement.¹⁰ The isotropic 2u octupole seems to contradict with experimental results. Note here that the pure electronic model cannot stabilize the 5u octupole, since there is no mixing between 4u and 5u moments for the case of $n=5$ with the ground state multiplet characterized by $J=5/2$. To obtain the mixed multipoles of 4u magnetic and 5u octupole, it is essentially important to consider the electron-phonon coupling. It is not yet clarified that the dominant phonon mode in filled skutterudites is Jahn-Teller type with E_g symmetry, but in any case, the effect of rattling seems to play a crucial role for the appearance of the octupole state. It may be interesting to carry out an experiment to detect a coupling between rattling and f -electron state in $\text{SmRu}_4\text{P}_{12}$.

Concerning the mechanism of magnetically robust heavy-fermion phenomena observed in $\text{SmOs}_4\text{Sb}_{12}$,¹⁷ a potential role of phonons has been pointed out from the viewpoint of the Kondo effect with non-magnetic origin.²⁰ In this context, the quasi-Kondo behavior due to the dynamical JT phonons may be a possible candidate to understand magnetically robust heavy-fermion phenomenon. Further investigations are required, in particular, concerning an experimental method to detect the Kondo-like behavior due to Jahn-Teller phonons. It is one of important future issues.

In summary, we have discussed the multipole state for the case of $n=5$ by analyzing the multipole Anderson model with the use of the NRG technique. When we do not consider the coupling between JT phonons and f electrons in Γ_{67}^- quartet, we have found that the dominant multipole moment is 2u octupole. When the coupling with JT phonons is switched and the cubic anharmonicity is included, the dominant multipole state is characterized by the mixture of 4u magnetic and 5u octupole moments, with significant fluctuations of quadrupole. We have also observed the quasi-Kondo behavior due to the entropy release concerning the rotational JT mode.

Acknowledgement

The author thanks Y. Aoki, H. Harima, K. Kubo, H. Onishi, Y. Nakanishi, and M. Yoshizawa for discussions. This

work has been supported by a Grant-in-Aid for Scientific Research in Priority Area “Skutterudites” under the contract No. 18027016 from the Ministry of Education, Culture, Sports, Science, and Technology of Japan. The author has been also supported by a Grant-in-Aid for Scientific Research (C) under the contract No. 18540361 from Japan Society for the Promotion of Science. The computation in this work has been done using the facilities of the Supercomputer Center of Institute for Solid State Physics, University of Tokyo.

- 1) *Proc. of 5th Int. Symposium on ASR-WYP-2005: Advances in the Physics and Chemistry of Actinide Compounds*, J. Phys. Soc. Jpn. (Suppl.) **75** (2006).
- 2) H. Sato, H. Sugawara, T. Namiki, S. R. Saha, S. Osaki, T. D. Matsuda, Y. Aoki, Y. Inada, H. Shishido, R. Settai and Y. Ōnuki: J. Phys.: Condens. Matter **15** (2002) S2063.
- 3) Y. Aoki, H. Sugawara, H. Harima and H. Sato: J. Phys. Soc. Jpn. **74** (2005) 209 (2005).
- 4) C. Sekine, T. Uchiyumi, I. Shirotni and T. Yagi: *Science and Technology of High Pressure*, ed. M. H. Manghnani, W. J. Nellis and M. F. Nicol, p. 826 (Universities Press, Hyderabad, India, 2000).
- 5) K. Matsuhira, Y. Hinatsu, C. Sekine, T. Togashi, H. Maki, I. Shirotni, H. Kitazawa, T. Takamasu and G. Kido: J. Phys. Soc. Jpn. (Suppl.) **71** (2002) 237.
- 6) C. Sekine, I. Shirotni, K. Matsuhira, P. Haen, S. De Brion, G. Chouteau, H. Suzuki and H. Kitazawa: Acta Phys. Pol. B **34** (2003) 983.
- 7) C. Sekine, Y. Shimaya, I. Shirotni and P. Haen, J. Phys. Soc. Jpn. **74** (2005) 3395.
- 8) K. Fujiwara, K. Ishihara, K. Miyoshi, J. Takeuchi, C. Sekine and I. Shirotni: Physica B **329-333** (2003) 476.
- 9) S. Masaki, T. Mito, N. Oki, S. Wada and N. Takeda, J. Phys. Soc. Jpn. **75** (2006) 053708.
- 10) M. Yoshizawa, Y. Nakanishi, M. Oikawa, C. Sekine, I. Shirotni, S. R. Saha, H. Sugawara and H. Sato: J. Phys. Soc. Jpn. **74** (2005) 2141.
- 11) K. Hachitani, H. Fukazawa, Y. Kohori, I. Watanabe, C. Sekine and I. Shirotni: Phys. Rev. B **73** (2006) 052408.
- 12) K. Hachitani, H. Amanuma, H. Fukazawa, Y. Kohori, K. Koyama, K. Kumagai, C. Sekine and I. Shirotni: to appear in J. Phys. Soc. Jpn.
- 13) K. Matsuhira, Y. Doi, M. Wakeshima, Y. Hinatsu, H. Amitsuka, Y. Shimaya, R. Giri, C. Sekine and I. Shirotni: J. Phys. Soc. Jpn. **74** (2005) 1030.
- 14) T. Hotta: J. Phys. Soc. Jpn. **74** (2005) 1275.
- 15) K. Takegahara, H. Harima and A. Yanase: J. Phys. Soc. Jpn. **70** (2001) 1190; *ibid.* **70** (2001) 3468; *ibid.* **71** (2002) 372.
- 16) Y. Nakanishi, T. Tanizawa, T. Fujino, H. Sugawara, D. Kikuchi, H. Sato and M. Yoshizawa: J. Phys. Soc. Jpn. (Suppl.) **75** (2006) 192.
- 17) S. Sanada, Y. Aoki, H. Aoki, A. Tsuchiya, D. Kikuchi, H. Sugawara and H. Sato, J. Phys. Soc. Jpn. **74** (2005) 246.
- 18) W. M. Yuhasz, N. A. Frederick, P.-C. Ho, N. P. Butch, B. J. Taylor, T. A. Sayles, M. B. Maple, J. B. Betts, A. H. Lacerda, P. Rogl and G. Giester: Phys. Rev. B **71** (2005) 104402.
- 19) Y. Aoki, S. Sanada, H. Aoki, D. Kikuchi, H. Sugawara and H. Sato: Physica B **378-380** (2006) 54.
- 20) S. Yotsuhashi, M. Kojima, H. Kusunose and K. Miyake: J. Phys. Soc. Jpn. **74** (2005) 49.
- 21) J. Kondo: Physica B+C (Amsterdam) **84** (1976) 40.
- 22) J. Kondo: Physica B+C (Amsterdam) **84** (1976) 207.
- 23) K. Hattori, Y. Hirayama and K. Miyake: J. Phys. Soc. Jpn. **74** (2005) 3306.
- 24) K. Hattori, Y. Hirayama and K. Miyake: J. Phys. Soc. Jpn. (Suppl.) **75** (2006) 238.
- 25) K. Kaneko, N. Metoki, T. D. Matsuda and M. Kohgi: J. Phys. Soc. Jpn. **75** (2006) 034701.
- 26) T. Goto, Y. Nemoto, K. Sakai, T. Yamaguchi, M. Akatsu, T. Yanagisawa, H. Hazama, K. Onuki, H. Sugawara and H. Sato: Phys. Rev. B **69** (2004) 180511(R).
- 27) T. Hotta: Physica B **378-380** (2006) 51.
- 28) T. Hotta: Phys. Rev. Lett. **95** (2006) 197201.
- 29) T. Hotta and H. Harima: J. Phys. Soc. Jpn. **75** (2006) No. 12, in press (cond-mat/0602646).
- 30) J. C. Slater: Phys. Rev. **34** (1929) 1293.
- 31) E. U. Condon and G. H. Shortley: Phys. Rev. **37** (1931) 1025.
- 32) J. A. Gaunt: Phil. Trans. Roy. Soc. **A228** (1929) 195.
- 33) G. Racah: Phys. Rev. **62** (1942) 438.
- 34) M. T. Hutchings: Solid State Phys. **16** (1964) 227.
- 35) K. R. Lea, M. J. M. Leask and W. P. Wolf: J. Phys. Chem. Solids **23** (1962) 1381.
- 36) T. Hotta and K. Ueda: Phys. Rev. B **67** (2003) 104518.
- 37) T. Hotta: Rep. Prog. Phys. **69** (2006) 2061.
- 38) T. Takimoto, T. Hotta, T. Maehira and K. Ueda: J. Phys.: Condens. Matter **14** (2002) L369.
- 39) T. Takimoto, T. Hotta and K. Ueda: J. Phys.: Condens. Matter. **15** (2003) S2087.
- 40) T. Takimoto, T. Hotta and K. Ueda: Phys. Rev. B **69** (2004) 104504.
- 41) T. Hotta and K. Ueda: Phys. Rev. Lett. **92** (2004) 107007.
- 42) T. Hotta: Phys. Rev. B **70** (2004) 054405.
- 43) H. Onishi and T. Hotta: New J. Phys. **6** (2004) 193.
- 44) T. Hotta: Phys. Rev. Lett. **94** (2005) 067003.
- 45) K. Kubo and T. Hotta: J. Phys. Soc. Jpn. **75** (2006) 083702.
- 46) K. Kubo and T. Hotta: Phys. Rev. B **71** (2005) 140404(R).
- 47) K. Kubo and T. Hotta: Phys. Rev. B **72** (2005) 144401.
- 48) K. Kubo and T. Hotta: Phys. Rev. B **72** (2005) 132411.
- 49) K. Kubo and T. Hotta: Physica B **378-380** (2006) 1081.
- 50) K. Kubo and T. Hotta: J. Phys. Soc. Jpn. (Suppl.) **75** (2006) 232.
- 51) H. Onishi and T. Hotta: J. Phys. Soc. Jpn. (Suppl.) **75** (2006) 266.
- 52) Y. Aoki, T. Namiki, S. Ohsaki, S. R. Saha, H. Sugawara and H. Sato: J. Phys. Soc. Jpn. **71** (2002) 2098.
- 53) T. Tayama, T. Sakakibara, H. Sugawara, Y. Aoki and H. Sato: J. Phys. Soc. Jpn. **72** (2003) 1516.
- 54) M. Kohgi, K. Iwasa, M. Nakajima, N. Metoki, S. Araki, N. Bernhoeft, J.-M. Mignot, A. Gukasov, H. Sato, Y. Aoki and H. Sugawara: J. Phys. Soc. Jpn. **72** (2003) 1002.
- 55) K. Kuwahara, K. Iwasa, M. Kohgi, K. Kaneko, S. Araki, N. Metoki, H. Sugawara, Y. Aoki and H. Sato: J. Phys. Soc. Jpn. **73** (2004) 1438.
- 56) E. A. Goremychkin, R. Osborn, E. D. Bauer, M. B. Maple, N. A. Frederick, W. M. Yuhasz, F. M. Woodward and J. W. Lynn: Phys. Rev. Lett. **93** (2004) 157003.
- 57) T. Hotta: to appear in J. Magn. Magn. Mater. (cond-mat/0610502).
- 58) P.-C. Ho, W. M. Yuhasz, N. P. Butch, N. A. Frederick, T. A. Sayles, J. R. Jeffries, M. B. Maple, J. B. Betts, A. H. Lacerda, P. Rogl and G. Giester: Phys. Rev. B **72** (2005) 094410.
- 59) K. W. H. Stevens: Proc. Roy. Soc. (London) **65** (1952) 209.
- 60) H. Harima and K. Takegahara: J. Phys.: Condens. Matter **15** (2003) S2081.
- 61) H. Harima, K. Takegahara, S. H. Curnoe and K. Ueda: J. Phys. Soc. Jpn. (Suppl.) **71** (2002) 70.
- 62) T. Hotta: J. Phys. Soc. Jpn. **74** (2005) 2425.
- 63) R. Shiina, H. Shiba and P. Thalmeier: J. Phys. Soc. Jpn. **66** (1997) 1741.
- 64) K. Kubo and T. Hotta: J. Phys. Soc. Jpn. **75** (2006) 013702.
- 65) K. G. Wilson: Rev. Mod. Phys. **47** (1975) 773.
- 66) H. R. Krishna-murthy, J. W. Wilkins and K. G. Wilson: Phys. Rev. B **21** (1980) 1003.